



Photorefractive two beam coupling characterization of a Barium-Calcium titanate crystal

Sylvie Bernhardt, Philippe Delaye, H. Veenhuis, D. Rytz, Gérald Roosen

► To cite this version:

Sylvie Bernhardt, Philippe Delaye, H. Veenhuis, D. Rytz, Gérald Roosen. Photorefractive two beam coupling characterization of a Barium-Calcium titanate crystal. Applied Physics B - Laser and Optics, 2000, 70, pp.789-795. 10.1007/s003400050010 . hal-00686038

HAL Id: hal-00686038

<https://hal-iogs.archives-ouvertes.fr/hal-00686038>

Submitted on 6 Apr 2012

HAL is a multi-disciplinary open access archive for the deposit and dissemination of scientific research documents, whether they are published or not. The documents may come from teaching and research institutions in France or abroad, or from public or private research centers.

L'archive ouverte pluridisciplinaire **HAL**, est destinée au dépôt et à la diffusion de documents scientifiques de niveau recherche, publiés ou non, émanant des établissements d'enseignement et de recherche français ou étrangers, des laboratoires publics ou privés.

Photorefractive two beam coupling characterization of a Barium-Calcium Titanate Crystal

Sylvie Bernhardt⁽¹⁾, Philippe Delaye⁽¹⁾, Holger Veenhuis⁽²⁾, Daniel Rytz⁽³⁾, Gérald Roosen⁽¹⁾

⁽¹⁾ Laboratoire Charles Fabry de l'Institut d'Optique, Unité Mixte de Recherche 8501 du Centre National de la Recherche Scientifique, Bat. 503, Centre Scientifique d'Orsay, B.P. 147, 91403 Orsay Cedex, France.

⁽²⁾ Universität Osnabrück, FachBereich Physik, D 49069 Osnabrück, Germany

⁽³⁾ Forschungsinstitut für Mineralische und Metallische Werkstoffe Edelsteine / Edelmetalle GMBH, Struthstr. 2, Wackenmühle, 55743 Idar-Oberstein, Germany

Corresponding Author : Ph. Delaye, Tel : 33 1 69358750, Fax : 33 1 69358700, Email :
Philippe.delaye@iota.u-psud.fr

Abstract: We present two beam coupling characterization of $\text{Ba}_{0.77}\text{Ca}_{0.23}\text{TiO}_3$, a ferroelectric material with no phase transition around room temperature that shows high photorefractive gain (7cm^{-1} with ordinary polarization and 15cm^{-1} with extraordinary polarization). We measure the electrooptic coefficients of $\text{Ba}_{0.77}\text{Ca}_{0.23}\text{TiO}_3$. These values are compared to estimated theoretical values, calculated using a model that allows to deduce the tetragonal phase parameter (Pockels and piezoelectrics coefficients) from the parameters of the high temperature cubic phase (Kerr and electrostriction coefficients).

PACS : 42.65.Hw, 77.84.-S

BaTiO₃ is a widely used photorefractive crystal. It possesses high electrooptic coefficients and thus exhibits a high photorefractive gain necessary for the implementation of phase conjugate mirrors. Nevertheless it suffers from a drawback that prevents its use in industrial systems, a phase transition from the tetragonal phase (4mm symmetry) towards an orthorhombic phase (mm2 symmetry) located at about 5°C. Passing this transition depolarizes the crystal and eventually causes its destruction. Recently, Ba_{0.77}Ca_{0.23}TiO₃ (BCT), a derivative of BaTiO₃ that presents this phase transition at a much lower temperature, was successfully grown [1]. This crystal was shown to be photorefractive [2], and thus presents a promising alternative to BaTiO₃ in photorefractive applications, provided that photorefractive performances are similar. At present time, very little is known about this new crystal and its photorefractive properties. The aim of this paper is to present some theoretical estimations of the characteristics of BCT and to compare them with experimental data. We first develop a theoretical approach in order to estimate the value of the effective electrooptic coefficients (as well as to evaluate the piezoelectric, elastic and elastooptic contributions) from the data (Kerr coefficients, electrostriction coefficients,...) of the material in the high temperature cubic phase (m3m symmetry). The model shows that rather high values of electrooptic coefficients are expected, even if it shows that the r_{42} parameter is reduced compared to BaTiO₃. Then we compare these theoretical values to the experimental ones deduced from two-beam coupling experiments performed in a 100ppm rhodium doped BCT at the wavelength of 532nm. These measurements show that high photorefractive gain values are obtained.

1. THEORETICAL BACKGROUND

At room temperature, BCT has the same symmetry than BaTiO₃. We will thus carry exactly the same kind of study on this new crystal as the one performed in baryum titanate. We thus perform classical measurements of the dependence of the photorefractive gain Γ with the grating wave number k_r . Γ is related to the electrooptic coefficients of the crystal in a way that depends on the geometrical configuration and polarization. This configuration is determined by two angles θ and β , where 2θ is the angle between the two incident beams inside the crystal and β is the angle between the grating wave vector and the optical axis (c-axis) inside the crystal (Figure 1).

We have chosen three simple configurations in order to determine the three non zero electrooptic coefficients of the crystal, i.e. $r_{113} = r_{223}$, r_{333} and $r_{131} = r_{232}$ (in contracted notation, $r_{13} = r_{23}$, r_{33} and $r_{51} = r_{42}$ respectively).

1.1. General definition of the effective electrooptic coefficient

For photorefractive crystals as BaTiO₃ and BCT, the change in the optic ellipsoid induced by the electric field is written as [3] :

$$\Delta\left(\frac{1}{n^2}\right)_{ij} = r_{ijk}^s E_k + p_{ijkl}^E u_{kl} \quad (1)$$

with

$$p_{ijkl}^E = p_{ijkl}^E + p_{ij[kl]}^E \quad (2)$$

where r_{ijk}^S is the clamped electrooptic coefficient, u_{kl} is the displacement gradient matrix of the deformation of the crystal induced by the piezoelectric effect, p_{ijkl}^E the elasto optic coefficients at constant field and $p_{ij[kl]}^E$ is the rotooptic effect. However, in BaTiO₃, the rotooptic contribution is rather small [5]. Therefore $[p'^E]$ can be assimilated to $[p^E]$ for BaTiO₃ (the same approximation will be made for BCT). After calculating the deformation u_{kl} produced by the space charge electric field $E = E_{sc} \cos(\vec{k}_r \cdot \vec{r})$, we have :

$$\Delta\left(\frac{1}{n^2}\right)_{ij} = r_{ij}^{eff} E_{sc} \cos(\vec{k}_r \cdot \vec{r}) = (r_{ijk}^S n_k E_{sc} + p_{ijkl}^E n_l A_{km}^{-1} B_m E_{sc}) \cos(\vec{k}_r \cdot \vec{r}) \quad (3)$$

with

$$A_{ik} = c_{ijkl}^E n_j n_l \text{ and } B_i = e_{kij} n_k n_j \quad (4)$$

where \vec{n} is a unit vector parallel to E_{sc} . c_{ijkl}^E is the elastic stiffness at constant field and e_{ijk} the piezoelectric coefficient.

As we can see, we do not use directly the classical electro-optic coefficients (r_{13} , r_{33} or r_{42}) but the effective electro-optic coefficients r_{11}^{eff} (which mainly corresponds to r_{113}), r_{22}^{eff} (which mainly corresponds to r_{223}), r_{33}^{eff} (connected to r_{333}) and r_{13}^{eff} (mainly related to r_{131}), that contain the elasto-optic contribution.

These expressions allow the calculation of the refractive index change due to the space charge field, that will depend on the respective orientation of the grating vector compared to the cristallographic axis and especially the c-axis.

1.2. Photorefractive gain

The space charge field is induced by the illumination grating pattern created by the interference of a pump beam and a signal beam. They create an index grating on which they diffract. This gives the possibility to induce an energy transfer from the pump beam towards the signal beam. This energy transfer is characterized by the photorefractive gain Γ that is expressed as [4] :

$$\Gamma = \frac{2\pi}{\lambda_0} n^3 r^{eff} E_{sc} (\hat{e}_s \cdot \hat{e}_p) \quad (5)$$

where λ_0 is the wavelength of light in vacuum, n the mean refractive index, E_{sc} the amplitude of the space-charge field and $(\hat{e}_s \cdot \hat{e}_p)$ the scalar product between the unit vectors which are aligned parallel to the electric field of the two beams. The dependence of Γ with the grating wave number k_r comes from E_{sc} [4] :

$$E_{sc} = \frac{k_B T}{e} \frac{k_r}{1 + (k_r/k_0)^2} \quad (6)$$

with k_0 that depends on the effective trap density N_{eff} :

$$k_0^2 = \frac{e^2 N_{eff}}{k_B T \epsilon_0 \epsilon^{eff}(\beta)} \quad (7)$$

The grating wave number is $k_r = 4\pi n \sin \theta / \lambda_0$ and $\epsilon^{\text{eff}}(\beta)$ is the effective dielectric constant which can be calculated from the clamped dielectric components ϵ_{ij}^S taking into account the elastic and piezoelectric contributions as for r^{eff} . Indeed, we have [5]

$$\epsilon^{\text{eff}} = \epsilon_{ij}^S n_i n_j + \epsilon_0^{-1} e_{ijk} e_{mnl} n_i n_j n_m n_n A_{kl}^{-1} \quad (8)$$

The scalar product (\hat{e}_s, \hat{e}_p) depends on the polarizations only and takes the values 1 or $\cos(2\theta)$ whether the light is ordinary or extraordinary polarized.

r^{eff} depends on the configuration and the polarizations. The expressions of r^{eff} for ordinary and extraordinary polarized light are respectively [5] :

$$r_0^{\text{eff}} = r_{22}^{\text{eff}}(\beta) \quad (9)$$

$$r_e^{\text{eff}} = \frac{1}{2} \left[r_{11}^{\text{eff}}(\beta) (\cos(2\theta) - \cos(2\beta)) + 2r_{13}^{\text{eff}}(\beta) \sin(2\beta) + r_{33}^{\text{eff}}(\beta) (\cos(2\theta) + \cos(2\beta)) \right] \cos(\beta) \quad (10)$$

1.3. Expression of the effective electrooptic coefficients in different experimental configurations

In the general case, the theoretical expression of r^{eff} is very complicated and depends on the different electrooptic coefficients (especially for the extraordinary polarization). We thus have studied specific configurations only, where the expression of the effective electrooptic coefficient is more simple, and the contribution of the different electrooptic coefficients can be separated. In most of the following we will now use the contracted tensorial notation [6], except when specified.

1.3.a. Determination of r_{13}^S and r_{33}^S

The simplest and easiest configuration is the one where the grating vector is along the c-axis (i.e. $\beta=0$). Then, r_0^{eff} and r_e^{eff} depend only on $r_{ii}^{\text{eff}}(0)$ that equals (Eq.3) [7] :

$$r_{ii}^{\text{eff}}(0) = r_{i3}^S + \frac{p_{i3}^E e_{33}}{c_{33}^E} \quad (11)$$

where the index i takes the value of 1 to 3. With this orientation, the effective dielectric constant is expressed as :

$$\epsilon^{\text{eff}}(0) = \epsilon_{33}^S + \frac{e_{33}^2}{c_{33}^E \epsilon_0} \quad (12)$$

If beams are ordinary polarized, we measure $r_{22}^{\text{eff}}(0)$, which can be related to the clamped electrooptic coefficient r_{23}^S :

$$r_{22}^{\text{eff}}(0) = r_{23}^S + \frac{p_{23}^E e_{33}}{c_{33}^E} \quad (13)$$

As $r_{23}^S = r_{13}^S$ and $p_{23}^E = p_{13}^E$, we have :

$$r_{22}^{\text{eff}}(0) = r_{23}^S + \frac{p_{23}^E e_{33}}{c_{33}^E} = r_{13}^S + \frac{p_{13}^E e_{33}}{c_{33}^E} = r_{11}^{\text{eff}}(0) \quad (14)$$

If beams are extraordinary polarized, the effective electrooptic coefficient equals to (using Eq.10) :

$$r_e^{\text{eff}} = (\cos(2\theta) - 1)r_{11}^{\text{eff}}(0) + (\cos(2\theta) + 1)r_{33}^{\text{eff}}(0) \quad (15)$$

As we know $r_{11}^{\text{eff}}(0)$ from the measurement with ordinary polarizations, we deduce $r_{33}^{\text{eff}}(0)$. It can be related to the clamped electro-optic coefficient r_{33}^S according to Eq.3 :

$$r_{33}^{\text{eff}}(0) = r_{33}^S + \frac{p_{33}^E e_{33}}{c_{33}^E} \quad (16)$$

Thus, two experiments conducted in the symmetrical configuration with the light polarized whether ordinary or extraordinary allow to determine $r_{22}^{\text{eff}} (=r_{11}^{\text{eff}})$ and r_{33}^{eff} , from which we deduce r_{13}^S and r_{33}^S respectively.

1.3.b. Determination of r_{42}^T

From Eq.10, the clamped electrooptic coefficient $r_{131}^S = r_{51}^S = r_{42}^S$ contributes to r_e^{eff} for $\beta \neq 0$ only. To determine this coefficient, we have to carry out experiments with extraordinary polarized light and with $\beta \neq 0$, that is to say in a non symmetrical configuration.

The crystal used, being cut along the crystallographic axes, we can only carry out measurements with β around 0 or $\pi/2$. But, for both values, there is no contribution of r_{13}^{eff} in r_e^{eff} because $\sin(2\beta) = 0$. If r_e^{eff} equals 0 when β equals $\pi/2$ ($\cos(\beta) = 0$), r_e^{eff} and thus Γ differ from zero as soon as β differs from $\pi/2$. The slope of the gain around $\pi/2$ is important, whereas the slope equals zero around $\beta = 0$. Thus, measuring the slope of the variation of the gain around $\beta = \pi/2$ will give an accurate measurement of r_{42}^S . Indeed, this slope is in first approximation proportional to r_{42}^T . Actually, this slope is proportional to the sum of $4 \times r_{42}^T$ and another term δ_r that depends on elastooptic, piezoelectric and elastic coefficients. This term is much smaller than $4 \times r_{42}^T$ for BaTiO₃ and we here suppose that it would be the same for BCT.

Moreover, to extract the electrooptic coefficient from this measurement, we must take into account the value of the effective dielectric constant that changes as we go from the low ϵ_{33} value to the high ϵ_{11} value, when β goes from 0 to $\pi/2$. From Eq.7, we need the value of $\epsilon^{\text{eff}}(\pi/2)$ which is given by Eq.8 as :

$$\epsilon^{\text{eff}}(\pi/2) = \epsilon_{11}^S + \frac{e_{15}^2}{c_{55}^E \epsilon_0} = \epsilon_{11}^T \quad (17)$$

So we are able to estimate r_{42}^T , itself connected to the clamped electrooptic coefficient r_{42}^S [7]:

$$r_{42}^T = r_{42}^S + \frac{p_{55}^E e_{15}}{c_{55}^E} \quad (18)$$

Thus, three simple experiments allow us to determine the three electrooptic coefficients of the BCT crystal, or at least the effective electrooptic coefficients that really appear in the determination of the photorefractive gain. Most of the parameters used (especially the piezoelectric and elastooptic

coefficients) are not known for BCT that is a rather new kind of materials. Nevertheless, it would be interesting to have an order of magnitude of their theoretical values to compare them to the parameters that will be measured. One method would have been to take for the unknown parameters the ones of BaTiO₃, but it leads to some inconsistency in the results. We prefer another method for this estimation, that allows to calculate the parameters in the tetragonal phase from the parameters of the high temperature cubic phase. The derived values would be closer to reality, as parameters such as the dielectric constants that are known to be different in BCT and in BaTiO₃ appears in the expressions. We will now describe this model.

2. THEORETICAL DETERMINATION OF THE PARAMETERS OF BCT

Above about 100°C, BaTiO₃ and BCT are in a cubic phase (m3m symmetry) and when the temperature decreases, they go into a tetragonal phase (4mm) (until 5°C for BaTiO₃ and down to at least -120°C for BCT). During this phase change, a spontaneous polarization P_s appears, that will bias the third order effects (as Kerr effect and electrostriction) to transform them into second order effects (Pockels effect and piezoelectric effect, respectively) [8]. We first apply the model to the BaTiO₃, in which all the parameters are known, in order to validate it, before applying it to BCT.

2.1. Determination of the parameters in the quadratic phase from the cubic phase parameters

2.1.a. Electrooptic effect

The electrooptic coefficients can be calculated from the quadratic Kerr coefficients in the cubic phase and from the spontaneous polarization for all the perovskites [9].

Considering the change of the optical permittivity tensor with electrical force and mechanical influence, we obtain the following relations between the clamped electro-optic coefficients r_{ij}^S and the clamped Kerr coefficients g_{ij}^S [9, 10] :

$$\begin{cases} r_{13}^S = r_{23}^S = 2g_{12}^S \epsilon_0 (\epsilon_{33}^S - 1) P_s \\ r_{33}^S = 2g_{11}^S \epsilon_0 (\epsilon_{33}^S - 1) P_s \\ r_{42}^S = r_{51}^S = 2g_{44}^S \epsilon_0 (\epsilon_{11}^S - 1) P_s \end{cases} \quad (19)$$

Knowing the total birefringence Δn_t is a sum of a polarization induced birefringence and a temperature-dependent structural contributions Δn_0 from the high-temperature phase [9], we calculate the value of the spontaneous polarization :

$$\Delta n_t = -\frac{1}{2} n^3 (g_{11}^S - g_{12}^S) P_s^2 + \Delta n_0(T) \quad (20)$$

The temperature-dependent structural term $\Delta n_0(T)$ is negligible for BaTiO₃ and consequently, we consider that it is the same for BCT

2.1.b. Piezoelectric and elastic stiffness coefficients

A treatment analogous to the one of [9] can be made in order to deduce the piezoelectric and elastic coefficients from the electrostrictive tensor [8].

We consider neither thermoelastic, nor electrothermal effects in the crystal. Forces applied to the crystal are stress σ and electric field E . The direct result of these forces are polarization P and strain τ . We take the nine stress components σ_{ij} and the polarization P_i as independent variables. Accordingly, we may write in tensorial notations for BaTiO₃ (or BCT) in the cubic state :

$$\tau_{ij} = s_{ijkl}^P \sigma_{kl} + Q_{ijkl}^\sigma P_k P_l \quad (21)$$

A spontaneous polarization appears in the tetragonal phase and introduces a first order piezoelectric effect. If we consider that the spontaneous polarization is along the z-axis, we have to replace P_3 by $(P_3 + P_s)$ and neglect all terms in P_1^2 , P_2^2 , P_3^2 and P_s^2 . Therefore, we have in tensorial notations :

$$\tau_{ij} = s_{ijkl}^P \sigma_{kl} + b_{kij} P_k \quad (22)$$

By comparing Eq.21 and 22, we find the piezoelectric coefficients b_{ij} in the tetragonal phase :

$$\begin{cases} b_{31} = b_{32} = 2Q_{12}P_s \\ b_{33} = 2Q_{11}P_s \\ b_{24} = b_{15} = Q_{44}P_s \end{cases} \quad (23)$$

Knowing that $d_{ij} = \epsilon_0 (\epsilon_{ik}^T - 1) b_{kj}$, we deduce the piezoelectric coefficients d_{ij}

$$\begin{cases} d_{31} = d_{32} = 2\epsilon_0 (\epsilon_{33}^T - 1) Q_{12}P_s \\ d_{33} = 2\epsilon_0 (\epsilon_{33}^T - 1) Q_{11}P_s \\ d_{15} = d_{24} = \epsilon_0 (\epsilon_{11}^T - 1) Q_{44}P_s \end{cases} \quad (24)$$

From the piezoelectric coefficients b_{ij} and d_{ij} and the elastic compliance at constant polarization s_{ij}^P (which is a parameter of the cubic phase), we calculate the elastic stiffness at constant electric field c_{ij}^E using the following relations [6, 7] :

$$s_{ij}^E = s_{ij}^P + b_{kl} d_{kj} \quad (25)$$

$$\tau_i = c_{ij}^E \sigma_j \quad \text{and} \quad \sigma_i = s_{ij}^E \tau_j \quad (26)$$

Then, we determine the piezoelectric tensor e_{ij} :

$$e_{ij} = d_{ik} c_{kj}^E \quad (27)$$

Finally we have a relation between the clamped ϵ_{ii}^S and unclamped ϵ_{ii}^T dielectric constants [7], in tensorial notation :

$$\epsilon_0 \epsilon_{ii}^S = \epsilon_0 \epsilon_{ii}^T - e_{ilm} d_{ilm} \quad (28)$$

2.1.c. Elastooptic effect

With an analogous reasoning as for the electrooptic coefficients, we find that the elastooptic coefficients at constant electric field p_{ij}^E depend on the quadratic electrooptic g_{ij}^S , piezoelectric e_{ij} , together with the spontaneous polarization P_S according to the following equation [10], in the tensorial notation :

$$p_{ijmn}^E = p_{ijmn}^P + 2(g_{ij3k}^S P_S) \cdot e_{kmn} \quad (29)$$

2.2. Theoretical values for all parameters

2.2.a. Necessary parameters of the cubic phase

From the model developed above, the basic parameters, that are necessary to calculate all the quadratic phase parameters, are :

- the unclamped dielectric constants ϵ_{ij}^T
- the clamped Kerr coefficients g_{ij}^S
- the elastooptic coefficients at constant polarization p_{ij}^P
- the electrostriction coefficients Q_{ij}
- the elastic compliance at constant polarization s_{ij}^P
- the total birefringence Δn_T and the mean refractive index n that will be used to calculate the spontaneous polarization P_S .

2.2.b. Validation of the model : case of the BaTiO₃

To validate the above developed modelisation, we first calculate the values of the quadratic phase parameters from the cubic phase parameters for BaTiO₃ and compare them to the values in the literature. We have listed the values of the needed coefficients of the cubic phase in Table 1. Table 2 shows the theoretical values found for BaTiO₃ as well as the experimental ones collected in Ref. [7]. The calculated values are in agreement with the published ones. The main difference is the value of the clamped dielectric constant ϵ_{33}^S which theoretical value is a factor of two higher (certainly connected to the smaller theoretical value of d_{33}). This difference is also present on the value of the electrooptic coefficient r_{13}^S and r_{33}^S that are directly proportional to ϵ_{33}^S . If we increase the value of Q_{11} (that governs d_{33} , see Eq.24) to $0.16\text{m}^4\text{C}^{-2}$, we obtain a better general accordance between the calculated values of the electrooptic coefficients and their experimental values.

With the different parameters given in Table 2 and using the theory of the first section, we are now able to calculate the theoretical values of the effective electrooptic coefficients that are experimentally measurable ($r_{22}^{\text{eff}}(0)$, $r_{33}^{\text{eff}}(0)$ and r_{42}^T). The results are presented in Table 3. The accordance between the theoretical values and the ones calculated from the experimental data of Table 2 is a little better than for the value of the electrooptic coefficient. This is probably due to a compensation of the different piezoelectric contributions, leading to a lesser influence of d_{33} that seems to be the critical parameter.

2.2.c. Application of the model : case of the BCT

Among the parameters of the cubic phase that we need to determine the whole set of parameters, some are known as the mean refractive index n and the total birefringence Δn_T [14] or the unclamped dielectric constants ϵ_{ij}^T [1]. Some are the same for all perovskites, as the clamped Kerr coefficients g_{ij}^S [9, 10], and some are unknown. In this last case, considering that the structure of BCT is closed to the one of BaTiO_3 , we use the coefficients of BaTiO_3 when those of BCT are missing. Table 4 is a summary of the values that we have used for the further calculations. The whole set of calculated parameters for BCT is presented in Table 5. Here again we can estimate the theoretical values of the effective electrooptic coefficients and of the effective dielectric constants (Table 6).

Compared to the case of BaTiO_3 , we remark that the values of r_{13}^S and r_{33}^S are higher for BCT, whereas r_{42}^S is smaller. This is evidently due to the higher value of ϵ_{33}^T and the smaller value of ϵ_{11}^T respectively. Further study will be necessary to determine the different parameters that are used in the calculation and refine the knowledge of the BCT crystal. Waiting for this determination, the model can nevertheless be used to predict the photorefractive performances of the BCT crystal.

3. EXPERIMENTAL RESULTS

Two-beam coupling measurements versus the grating wave vector are carried out for ordinary and extraordinary polarizations on a single domain $\text{Ba}_{0.77}\text{Ca}_{0.23}\text{TiO}_3$ crystal Rhodium doped at 100ppm. The dimensions of the sample are $a * b * c = 1.76 \text{ mm} * 4.74 \text{ mm} * 3.48 \text{ mm}$, where c is the optical axis. In all the experiments, we use a frequency-doubled Nd:YAG laser at 532 nm. From the steady state intensities of the transmitted weak signal beam without and with illumination by the pump beam, we calculate the two beam coupling coefficient. Each measurement datum corresponds to a measurement in attenuation and in amplification allowing to separate the photorefractive components from an eventual absorption component (induced absorption or absorption grating). In order to be sure that we saturate the photorefractive gain, we have measured the gain versus incident illumination. The criterion for saturation is that gain should not depend on illumination and we have selected a large enough value of the incident intensity to be saturated. From the measured values reported in Fig.2, the gain is constant as soon as the intensity is higher than 500 mW.cm^{-2} . It reaches half of its maximum for an intensity I_{sat} of 50 mW.cm^{-2} . All the following experiments have been performed with an intensity of 1.2 W.cm^{-2} .

3.1. Experiments around $\beta=0$

The experimental data (Fig.3) are adjusted with expression (5) and (6). The experiments are conducted with an angle $\beta=0$. From this fit, we determine, in ordinary polarization, the two parameters $r_{22}^{\text{eff}}(0) = (22 \pm 0.3) \text{ pm.V}^{-1}$ and $N_{\text{eff}} = (5.3 \pm 0.4) 10^{22} \text{ m}^{-3}$. The value of N_{eff} is determined using the value of $\epsilon^{\text{eff}}(0)$ calculated above. This value for N_{eff} is slightly different from the previously published value [15] because of a numerical error in the calculation of ϵ^{eff} used then in the extraction of N_{eff} from k_0 .

From Eq.15, the gain in extraordinary polarization with $\beta=0^\circ$ depends on $r_{11}^{\text{eff}}(0) = r_{22}^{\text{eff}}(0)$, $r_{33}^{\text{eff}}(0)$ and on N_{eff} . Consequently, we use the previously determined values of N_{eff} and of $r_{11}^{\text{eff}}(0) = r_{22}^{\text{eff}}(0)$, and

make an adjustment to deduce $r_{33}^{\text{eff}}(0) = (55 \pm 0.6) \text{ pm} \cdot \text{V}^{-1}$. To make this adjustment, we transform Eq.15 using the fact that $\cos(2\theta)$ can be written as a function of k_r .

3.2. Experiments around $\beta=\pi/2$

As explained previously, we performed experiments around $\beta=\pi/2$ and we deduced the value of r_{42}^T from the slope of the experimental curve. We used extraordinary polarized beams to carry out measurements versus β near the value of $\pi/2$. We fixed the grating spacing ($k_r = 8 \mu\text{m}^{-1}$) and thus the space charge field by Eq.6. In this configuration, it can be estimated using the value of N_{eff} and the theoretical value of $\varepsilon(\pi/2)$. A linear fit on our experimental points (Fig.4) gives the value of the slope from which we deduce $r_{42}^T = 250 \text{ pm} \cdot \text{V}^{-1}$. Using calculated values of Table 5, we have verified that the neglected term is effectively negligible ($\delta_r = 54 \text{ pm} \cdot \text{V}^{-1} \ll 4 \times r_{42}^T$) and would have lead to a less than 5% correction.

3.3. Discussion

A first conclusion is that the experimental values of the effective electrooptic coefficients (which are the ones we effectively use in the experiments) are quite strong and compare rather well with the theoretical values presented in Table 6. This is true even if we consider that the problem of the reduction of the gain, due to an eventual electron-hole competition, has not been taken into account in our study. In a first approximation, the action of the electron-hole competition is just to reduce the gain by a constant factor ξ_0 ($-1 < \xi_0 < 1$). If ever electron-hole competition exists in the crystal, the found values of the electrooptic coefficients have to be divided by ξ_0 . The found electrooptic values are thus lower limits of the real values.

4. CONCLUSION

We have presented in this paper a characterization of the two beam coupling photorefractive gain Γ in a photorefractive $\text{Ba}_{0.77}\text{Ca}_{0.23}\text{TiO}_3$ crystal. This crystal is derived from BaTiO_3 but has the advantage of not presenting the low temperature phase transition around 5°C . The study shows that high photorefractive gain can be obtain even with symmetric configurations (i.e. without using the r_{42} electrooptic coefficient). Indeed, photorefractive gain as high as 7 cm^{-1} with ordinary polarization and 15 cm^{-1} with extraordinary polarization have been measured at 532 nm . This corresponds to rather high effective electrooptic coefficients, at least comparable to the one of BaTiO_3 , if not higher. These values agree quite well to the theoretical values.

Using a model that allows to calculate the parameters of the crystal in the tetragonal phase from the ones in the cubic phase, we compared the measured effective electrooptic coefficients with their theoretical values. The order of magnitude of the parameters is respected, but for a better comparison, we will need to have a better knowledge of the BCT crystal, as for most of the cubic phase parameters of BCT, we take in a first approximation the value they have in BaTiO_3 . These first measurements are promising and confirm the interest of this new material for photorefractive applications, even if further characterizations are necessary.

REFERENCES

- [1] Ch.Kuper, R.Pankrath, H.Hesse. Appl. Phys. A. **65**, 301 (1997).
- [2] Ch.Kuper, K.Buse, U.Van Stevendaal, M.Weber, T.Leidlo, H.Hesse, E.Krätzig. Ferroelectrics **208-209**, 213 (1998).
- [3] P.Günter, M.Zgonik. Optics Letters **16**, 23 (1991)
- [4] N.V. Kukhtarev, V.B. Markov, S.G. Odulov, M.S. Soskin, V.L. Vinetskii. Ferroelectrics **22**, 949 (1979) and Ferroelectrics **22**, 961 (1979)..
- [5] M.Zgonik, K. Nakagawa, P.Günter. J. Opt. Soc. Am. B **12**, 1416 (1995).
- [6] J.F.Nye, "*Physical Properties of Crystals* " (Oxford University Press, 1957, 1985), pp. 170-191.
- [7] M.Zgonik, P.Bernasconi, M.Duelli, R.Schlessler, P.Günter, M.H.Garrett, D.Rytz, Y.Zhu, X.Wu. Phys.Rev.B **50**, 5941 (1994).
- [8] A.F.Devonshire. Phil.Mag. **42**, 1065 (1951).
- [9] M.DiDomenico Jr, S.H.Wemple. J. Appl. Phys. **40**, 720 (1969) and J. Appl. Phys. **40**, 735 (1969) .
- [10] P.Bernasconi, M.Zgonik, P.Günter. J. Appl. Phys. **78**, 2651 (1995).
- [11] E.J.Huibregtse, W.H.Bessey, M.E.Drougard. J. Appl. Phys. **30**, 899 (1959).
- [12] F.Jona, G.Shirane, "*Ferroelectric Crystals*" Pergamon Press, New York (1962).
- [13] K.Buse, S.Riehemann, S.Loheide, H.Hesse, F.Mersch, E.Krätzig. Phys. Status Solidi (a) **135**, K.87 (1993).
- [14] M.Simon, F.Mersch, C.Kuper, S.Mendricks, S.Webering, J.Imbrock, E.Krätzig. Phys. Stat. Sol. (a) **159**, 559 (1997).
- [15] S. Bernhardt, Ph.Delaye. H. Hesse, D. Rytz, G. Roosen. OSA Trends in Optics and Photonics, Advances in photorefractive Materials, Effects, and Devices, **27**, 132 (1999)

FIGURE CAPTIONS

Figure 1 : Orientation of the input beams and the crystal axis.

Figure 2 : Experimental photorefractive gain Γ versus illumination for a grating spacing of $0.6 \mu\text{m}$, an angle $\beta=0$ and an ordinary polarization.

Figure 3 : Experimental photorefractive gain Γ as a function of the grating spacing for ordinary and extraordinary polarizations.

Figure 4 : Experimental photorefractive gain Γ as a function of the angle between the grating wave vector and the \mathbf{c} -axis around ($\beta=\pi/2$).

TABLE CAPTIONS

Table 1 : Material coefficients in the cubic phase of the BaTiO_3 .

Table 2 : Numerical results for the whole set of parameters for BaTiO_3 , experimental values are taken from Ref. [7], except when precised.

Table 3 : Effective electrooptic coefficients for BaTiO_3

Table 4 : Material coefficients in the cubic phase of BCT.

Table 5: Numerical results for the whole set of parameters for BCT.

Table 6 : Effective electrooptic coefficients and dielectric constant for BCT

	Numerical values	Reference
$g_{11}^S (10^{-2}m^4.C^{-2})$	15 ± 3	[10]
$g_{12}^S (10^{-2}m^4.C^{-2})$	3.8 ± 0.6	[10]
$g_{44}^S (10^{-2}m^4.C^{-2})$	7 ± 1.5	[10]
p_{11}^P	0.37 ± 0.03	[10]
p_{12}^P	0.11 ± 0.01	[10]
p_{66}^P	-0.30 ± 0.15	[10]
$s_{11}^P (10^{-12}m^2.N^{-1})$	8.7	[11]
$s_{12}^P (10^{-12}m^2.N^{-1})$	-3.35	[11]
$s_{66}^P (10^{-12}m^2.N^{-1})$	8.9	[11]
$Q_{11} (m^4.C^{-2})$	0.09	[9, 12]
$Q_{12} (m^4.C^{-2})$	-0.04	[9, 12]
$Q_{44} (m^4.C^{-2})$	0.06	[9, 12]
Δn	0.07	[13]
n	2.49	[13]
ϵ_{11}^T	4450 ± 400	[7]
ϵ_{33}^T	129 ± 5	[7]

Table 1

	Experimental values	Calculated values
Spontaneous polarization (C.m ⁻²)		
P _S	0.28 [10]	0.28
Elastic stiffness at constant field (10 ¹⁰ N.m ⁻²)		
c ₁₁ ^E	22.3±1	22.1
c ₃₃ ^E	15.1±0.7	20.1
c ₁₂ ^E	10.9±1.8	13.8
c ₁₃ ^E	11.1±0.8	14.3
c ₄₄ ^E	5.9±0.3	5.0
c ₆₆ ^E	13.2±1.1	11.2
Piezoelectric coefficients (pm.V ⁻¹)		
d ₃₁	-33.4±2	-25.2
d ₃₃	90±4	57
d ₁₅	580±20	658
Piezoelectric coefficients (C.m ⁻²)		
e ₃₁	-0.70±0.6	-0.90
e ₃₃	6.60±0.3	4.20
e ₁₅	34.6±1.5	33
Elasto-optic coefficients at constant field		
p ₁₁ ^E	0.50±0.04	0.35
p ₁₂ ^E	0.106±0.01	0.09
p ₁₃ ^E	0.20±0.01	0.20
p ₃₁ ^E	0.07±0.006	0.03
p ₃₃ ^E	0.77±0.04	0.72
p ₄₄ ^E	0.98±0.16	0.99
p ₆₆ ^E	-	-0.30
Clamped dielectric constants		
ε ₁₁ ^S	2174±100	1986
ε ₃₃ ^S	56.4±3	97
Clamped electro-optic coefficients (pm.V ⁻¹)		
r ₁₃ ^S	10.2±0.6	18
r ₃₃ ^S	40.4±2	70.8
r ₄₂ ^S	730±100	342.3

Table 2

	Calculated from Table 2 values	Theoretical value
$r_{22}^{\text{eff}}(0)$	18.9 pm.V ⁻¹	22.2 pm.V ⁻¹
$r_{33}^{\text{eff}}(0)$	74 pm.V ⁻¹	86 pm.V ⁻¹
r_{42}^{T}	1300 pm.V ⁻¹	995 pm.V ⁻¹

Table 3

	Numerical values	Remark
$g_{11}^s (10^{-2}m^4.C^{-2})$	15 ± 3	Same for all the perovskites
$g_{12}^s (10^{-2}m^4.C^{-2})$	3.8 ± 0.6	
$g_{44}^s (10^{-2}m^4.C^{-2})$	7 ± 1.5	
p_{11}^p	0.37 ± 0.03	Values of BaTiO ₃
p_{12}^p	0.11 ± 0.01	
p_{66}^p	-0.30 ± 0.15	
$s_{11}^p (10^{-12}m^2.N^{-1})$	8.7	
$s_{12}^p (10^{-12}m^2.N^{-1})$	-3.35	
$s_{66}^p (10^{-12}m^2.N^{-1})$	8.9	
$Q_{11} (m^4.C^{-2})$	0.09	
$Q_{12} (m^4.C^{-2})$	-0.04	[14]
$Q_{44} (m^4.C^{-2})$	0.06	
Δn	0.05	
n	2.46	
ϵ_{11}^T	1120 ± 30	
ϵ_{33}^T	240 ± 10	[1]

Table 4

	Measured value	Calculated value
Spontaneous polarization (C.m ⁻²)		
P _S		0.26
Elastic stiffness at constant field (10 ¹⁰ N.m ⁻²)		
c ₁₁ ^E		22.1
c ₃₃ ^E		19.4
c ₁₂ ^E		13.8
c ₁₃ ^E		14.5
c ₄₄ ^E		8.9
c ₆₆ ^E		11.2
Piezoelectric coefficients (pm.V ⁻¹)		
d ₃₁		-43
d ₃₃		97
d ₁₅		151
Piezoelectric coefficients (C.m ⁻²)		
e ₃₁		-1.36
e ₃₃		6.25
e ₁₅		13.5
Elasto-optic coefficients at constant field		
p ₁₁ ^E		0.34
p ₁₂ ^E		0.08
p ₁₃ ^E		0.23
p ₃₁ ^E		0.01
p ₃₃ ^E		0.85
p ₄₄ ^E		0.18
p ₆₆ ^E		-0.30
Clamped dielectric constants		
ε ₁₁ ^S		888
ε ₃₃ ^S		158
Clamped electro-optic coefficients (pm.V ⁻¹)		
r ₁₃ ^S	36±3 [2]	27
r ₃₃ ^S	140±5 [2]	106
r ₄₂ ^S		140

Table 5

	Calculated value
$r_{22}^{\text{eff}}(0)$	34 pm.V ⁻¹
$r_{33}^{\text{eff}}(0)$	133 pm.V ⁻¹
r_{42}^{T}	168 pm.V ⁻¹
$\varepsilon(0)$	181
$\varepsilon(\pi/2)$	1120

Table 6

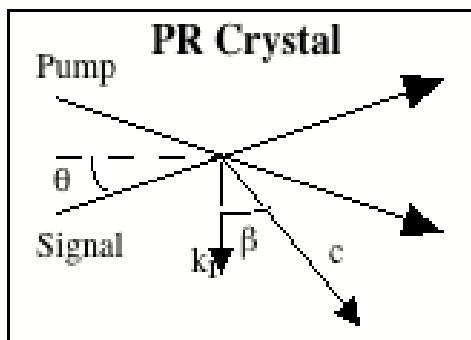


Figure 1

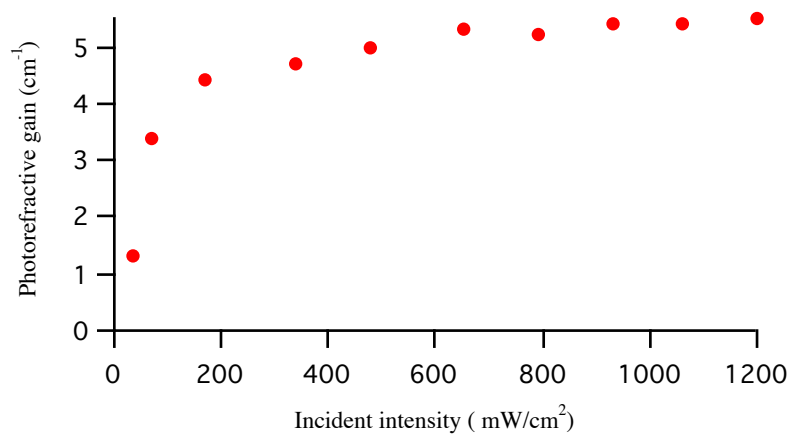


Figure 2

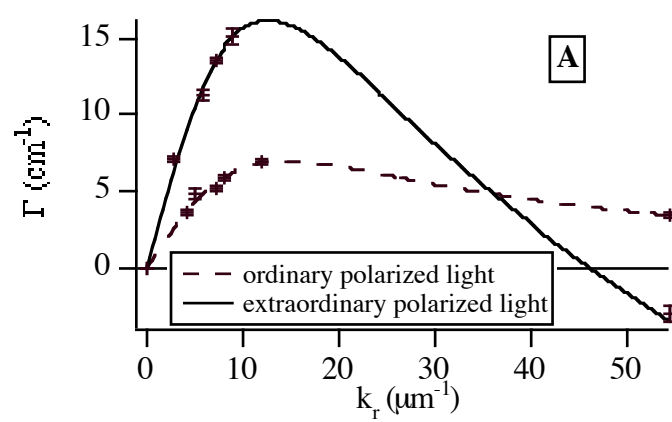


Figure 3

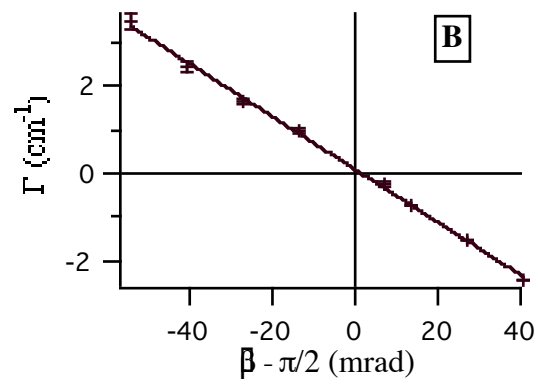


Figure 4